

# Characterization of an Artificially Prepared Cohesive Soil Bed

Z. Rehman<sup>1</sup>, A. Akbar<sup>2</sup> and B.G. Clarke<sup>3</sup>

<sup>1</sup>Ph.D. Student, Department of Civil Engineering, University of Engineering and Technology, Lahore-Pakistan

<sup>2</sup>Professor, Department of Civil Engineering, University of Engineering and Technology, Lahore-Pakistan

<sup>3</sup>Professor, Department of Civil Engineering Department, University of Leeds, UK

## Abstract

A new pressuremeter has been developed at the University of Engineering and Technology, Lahore-Pakistan with some modifications / improvements in the Newcastle full displacement pressuremeter (NFDPM), developed by Akbar in 2001. The device is now called Akbar Pressuremeter (APMT). Tests in soils can be performed using the APMT by full displacement as well as pre-bored techniques.

This paper describes the results of characterization of an artificially prepared cohesive soil bed comprising low plastic lean clay (CL) to sandy silty clay (CL-ML) using the APMT. This testing was carried out by pre-bored technique. For this purpose initially borehole produced up to the desired test level using auger and then device was inserted into the borehole to conduct the test. The pressuremeter (PMT) testing was carried out at two locations at 1.0 m intervals to 5.0 m depth. Undisturbed soil samples (UDS) were taken from nearby locations at the level of each APMT test using Shelby tubes. These samples were subjected to various conventional laboratory tests to correlate with the APMT test results. The standard penetration tests (SPTs) were also carried out in the near vicinity at the level of each APMT in order to correlate PMT data with the SPT data. Undrained shear strength of each UDS was determined by performing unconfined compression test.

The PMT parameters viz. soil strength and stiffness, determined from the corrected pressure-cavity strain curves of each APMT test and those from laboratory methods, have been compared and correlations have been drawn. The findings of this study are that the APMT can be used to characterize a cohesive soil bed.

**Key Words:** Pressuremeter; clay; SPT; shear strength; shear modulus; in-situ horizontal stress

## 1. Introduction

Subsoil investigation, consisting of in-situ tests either independently or in combination with laboratory tests, has become a prerequisite for any civil engineering project [1]. It provides cost-effective and safe design of the substructure elements [2]. While laboratory testing forms a crucial part of any subsoil exploration, in-situ testing has become progressively more enviable in order to obtain various soil parameters. Results can not be provided at the time of subsoil investigation with laboratory methods of testing soil samples, whether disturbed or undisturbed. Basically soils are first sampled at the site, transported to the laboratory and then tested for the determination of the required parameters. Anonymous and different soil disturbance can have impact on the soil fabric and can change the void ratio and density of the soil. The effect on these parameters can everlastingly change the strength and deformation properties of the soil specimens.

The growing ranges of design and construction problems and diversity of geological situations have led to the development of many in-situ test techniques [3]. In order to address these issues, geotechnical engineers have been trying to develop new in-situ soil testing devices and data analysis procedures around the world. These include cone penetrometers, pressuremeters, dilatometers etc. These devices have been developed to produce better quality soil parameters. However, such devices are sophisticated, hence expensive to buy or hire, making their use unaffordable on small projects.

The first pressuremeter of full-displacement type was developed by Withers et al. (1986) [4]. It is headed by a 15 cm<sup>2</sup> solid cone, which is pushed into place by displacing the ground. It measures the inflation pressure and the circumferential strain at three locations 120° apart at the centre of the membrane. A Chinese lantern, making the probe sophisticated, secures the membrane. The Fugro cone pressuremeter has been further simplified by the use of a volume change measurement system to measure the pressuremeter membrane expansion rather than using strain gauges. The assembly and test control have also been made easier [5] but the basic design has remained unchanged. While many efforts have been made to make it simpler, no effort has been made to measure the pressuremeter membrane expansion with a single transducer till 2001. Akbar [6] developed full-displacement pressuremeter keeping length of test section 420 mm [7], which is nearly the same as that of the *FDP*M, developed by Withers et al (1986) [4].

The *SPT* equipment was developed in the 1900's to determine the ability of the ground to support end-bearing piles. The blow count provides a measurement of the strength of the ground which led to many empirical correlations with laboratory determination of stiffness and strength or direct predictions of settlement and bearing capacity [8]. In Pakistan the geotechnical design parameters are being obtained by *SPT* testing in the field and laboratory testing on disturbed and undisturbed soil samples collected from the field. The *SPT*, though commonly used around the world, does not provide soil parameters of high quality. The

pressuremeter is believed to provide soil parameters of relatively better quality, particularly the stiffness of the soil [9]. The unavailability of such devices in developing countries like Pakistan give emphasis on the need to develop a new generation of cost-effective in-situ testing devices having ability to produce high quality geotechnical design parameters. The target design parameters are strength, stiffness and in-situ stress.

The research was, therefore, carried out to develop a relatively robust and simple version having ability to yield higher quality soil design parameters, with certain modifications to the design of Newcastle full-displacement pressuremeter (*NFDPM*) developed by Akbar in 2001. For the development of this new testing device most of the local resources have been used. Testing has been carried out using this new version of *NFDPM*. The new version of this device is called the Akbar pressuremeter (*APMT*). It is instrumented with transducers to measure expansion of the membrane and the pressure to expand it. The *SPT* blows are recorded for 305 mm penetration of the split spoon sampler. The length of the test section of the pressuremeter probe has been kept 305 mm, in order to correlate the pressuremeter data with the *SPT* blows. This similarity was intended to benefit from the long experience available on the *SPT*.

The aim of this study was to use the *APMT* by pre-bored technique and to check / improve correlations between the *APMT* indices, soil properties and geotechnical design parameters by performing tests on an artificially prepared cohesive soil bed. In order to correlate the *APMT* data with parameters obtained from other types of tests, undisturbed samples (*UDS*) were obtained using 38 mm

diameter Shelby tubes. The *UDS* were retrieved from the same depths as the *APMT* tests from two boreholes close to the pressuremeter test locations. Boreholes were advanced by augering and Shelby tubes were gently hammered into the soil to obtain relatively undisturbed soil samples. Tests were carried out on the *UDS* to determine undrained shear strength along with water content, unit weight and classification of soil.

## 2. Akbar Pressuremeter (*APMT*)

The main body of the probe of the *APMT* as shown in Figure 1 is made of high strength stainless steel. Its diameter is 44.4 mm with a 305 mm long test section (*L*). With the membrane in place, the outer diameter of the probe (*D*) is 48.2 mm. The *L/D* ratio is therefore 6.3. Both ends of the main body are identical. One end is connected to the pressure hose and the electrical cable by a re-usable hydraulic fitting. A 45° stainless steel cone having a maximum diameter of 50.8 mm (surface area 28.5 cm<sup>2</sup>) is screwed to the other end. The main body has a 115 mm long and 10 mm wide slot in the middle in Figure 1a for the expansion arms assembly (Figure 2). A longitudinal hole of 8 mm diameter is drilled from one end (the end to which the hydraulic coupling is connected) up to the central slot. This hole houses the transducer wires and transmits the pressurised gas, which inflates the membrane. The radial grooves have been machined to allow the dry nitrogen gas (*N*<sub>2</sub>) pressure to reach everywhere underneath the membrane simultaneously. This allows the whole length of the membrane to expand uniformly under uniform soil conditions around the probe.

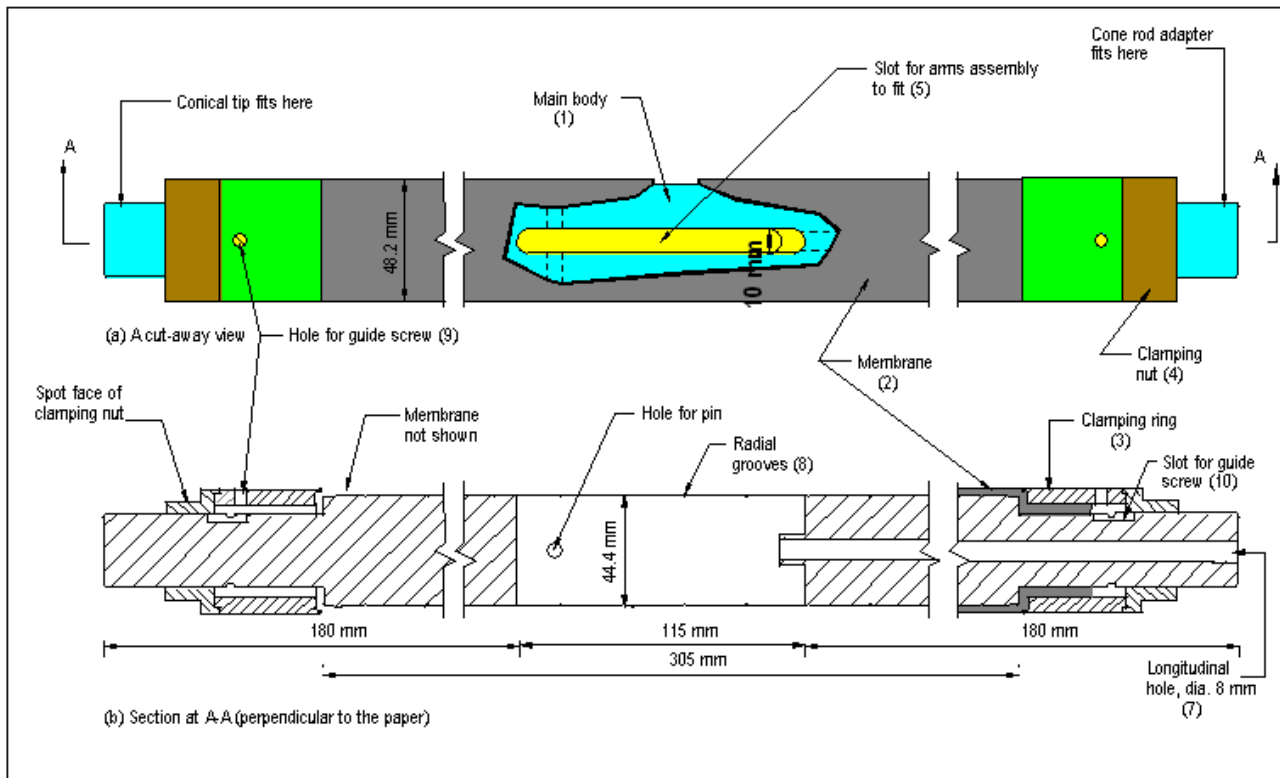


Fig. 1: Full-displacement pressuremeter probe.

Figure 2 shows the assembly of the expansion arms. The arms, made of stainless steel, move outward about a pivot point. The hair spring activates this outward movement. At zero expansion of the membrane, the distance between the outer surfaces of the arms is the same as that of the main body (i.e. 44.4 mm) as shown in Figure 2(a). The arms can move apart radially from 44.4 mm to a maximum of 66 mm). This limit is reached when the part of arm-1 containing magnet 2 comes in contact with the projecting part of the seat for the linear output Hall Effect Transducer (*HET*), as shown in Figure 2(b). The expansion of arms is about 45% according to this design. The *HET* has been glue mounted on its seat, positioning it between the two magnets located in arm-1. The expansion of the arms changes the

output of the *HET* mounted inside the arms as shown in Figure 3. The *HET* is connected to the A/D data-logger at the surface using an electrical cable, which passes through a pressure hose. One end of the pressure hose is permanently fixed to the pressuremeter probe while the other end is fixed to the gas-electric separator during in-situ testing. The gas-electric separator separates the cable and the hose and a pressure transducer fitted to it measures the gas pressure applied during the membrane expansion.

The pressuremeter membrane consists of two layers. The inner layer (2.20 mm thick) is made from Nitrile and is reinforced by encasing with a (1.10 mm thick) Nylon cover. The inside and outside diameters of the rubber membrane are 31.75 and 38.35 mm respectively.

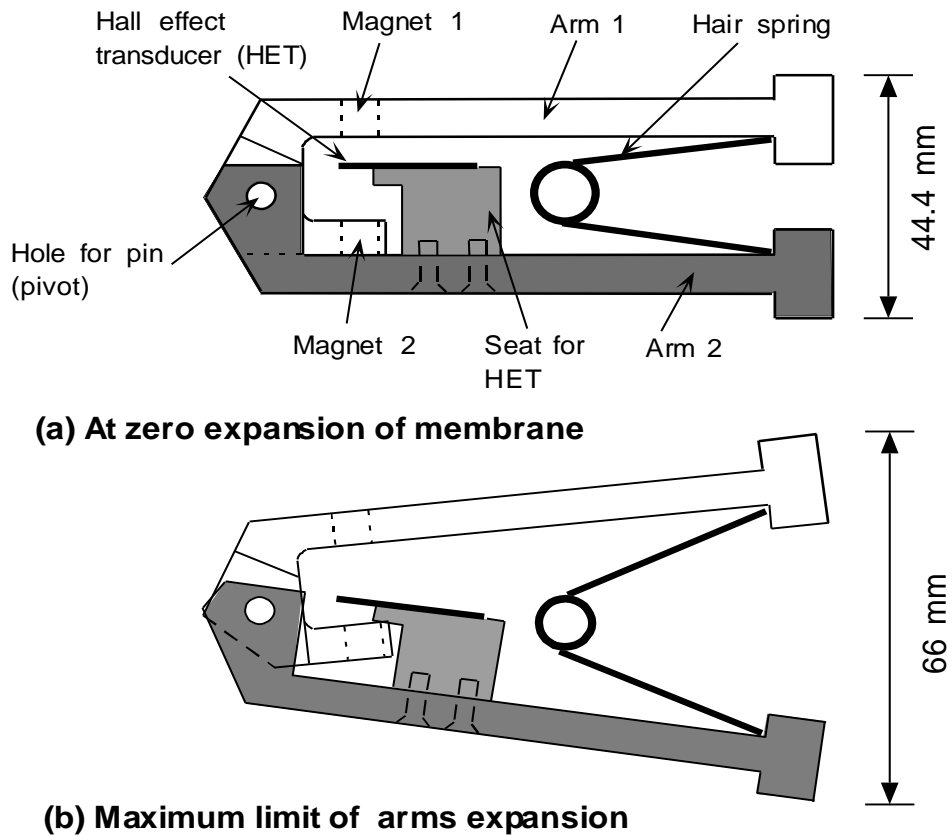
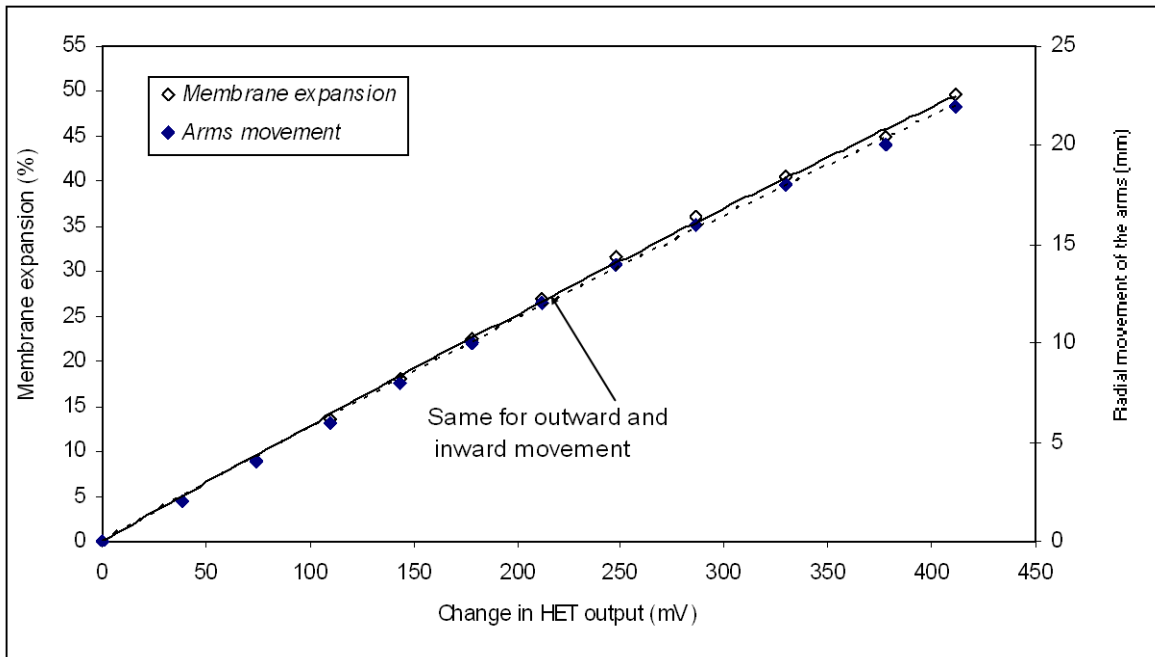
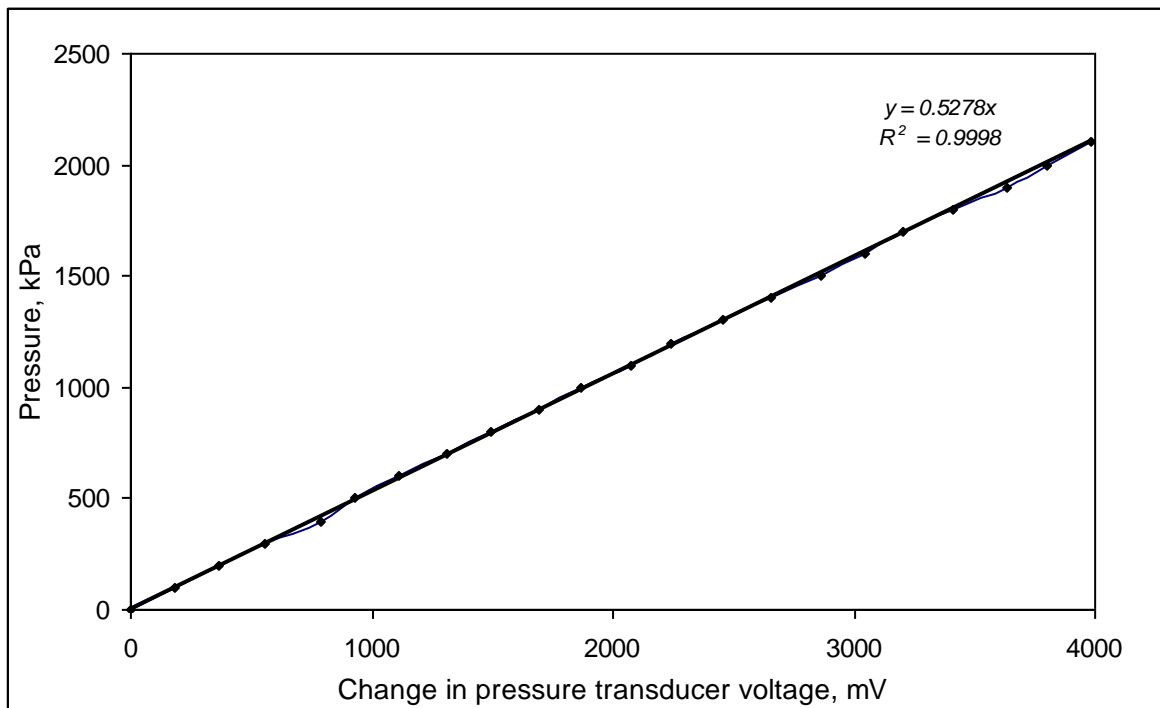


Fig. 2: Expansion arms [6].



**Fig. 3:** A typical calibration data plot for the *HET* in the *APMT*



**Fig.4:** A typical calibration data plot for pressure transducer.

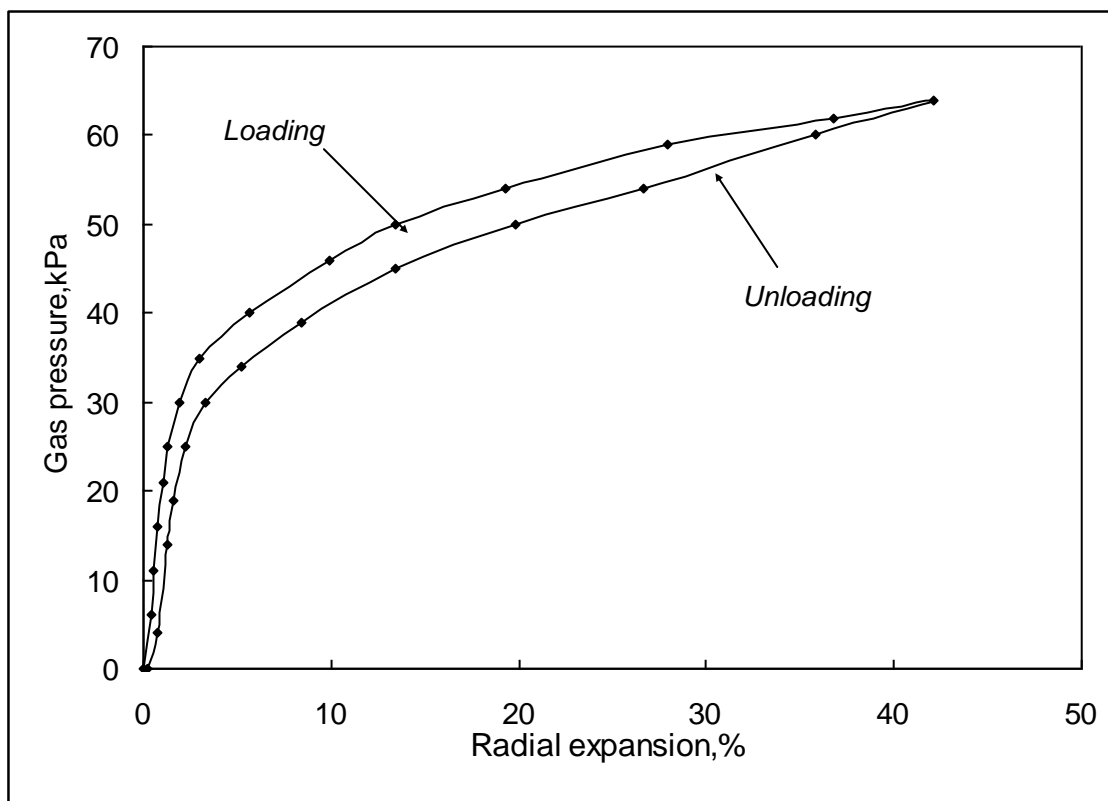


Fig. 5: A typical calibration data plot for radial expansion of the APMT membrane.

### 3. Calibration for System Stiffness

Three calibrations are required (i) *HET* for expansion measurement (ii) Pressure Transducer (iii) System stiffness. Calibration of *HET* is described earlier. The calibration of the pressure transducer was carried out using a Budenberg dead weight gauge. The calibration data for the pressure transducer used is plotted as shown in Figure 4. The calibration for membrane stiffness was carried out by increasing the gas pressure in small increments of about 10 kPa, maintaining each increment for 60 seconds. In 60 seconds, the radial expansion of the membrane was found to be almost complete. The same time duration is used for the Ménard pressuremeter test. When the arms had moved out to their maximum design distance (which was reflected by the constant output of the *HET*), unloading was commenced using similar decrements until full contraction of the arms. The radial expansion of the membrane in percentage was plotted against the gas pressure applied as shown in Fig.5.

### 4. Test Site

The APMT testing was carried out at an Open Area of the Civil Engineering Department, University of Engineering and Technology, Lahore-Pakistan. For this purpose, a test pit of size 3m x 3m and 5m deep was excavated and backfilled with a borrowed cohesive soil. The

ground water table is much lower than 5.0 m. During backfilling, the pit was kept filled with water and the borrow material was dropped from the surface into the pit manually. This technique was employed to obtain uniform moisture content and density conditions in the test pit. This methodology of soak filling also simulates the process through which natural deposits are usually formed. The APMT testing was carried out after a lapse of about one year to allow the soil to achieve equilibrium condition.

### 5. Field Testing

The equipment was assembled at the site as shown in the schematic sketch Figure 6. The APMT testing was carried out at two locations using pre-bored technique (*PB-1* and *PB-2*). The SPT and undisturbed sampling using 38 mm Shelby tubes were carried out in the nearby locations at the levels of APMT testing as per plan shown in Figure 7. The bore hole was created up to the desired test depth by an auger of 40 mm diameter and the APMT probe was put into the hole keeping the centre of the probe at a test level to carry out the APMT testing. An auger of 40 mm diameter was used as it created a bore hole diameter equal to about 50 mm. The diameter of the cone is 50.8 mm which means that cone in front of test section will just touch the wall of the hole during its lowering. Testing interval was kept as 1 m so that the previous one above should not affect a test. Stress

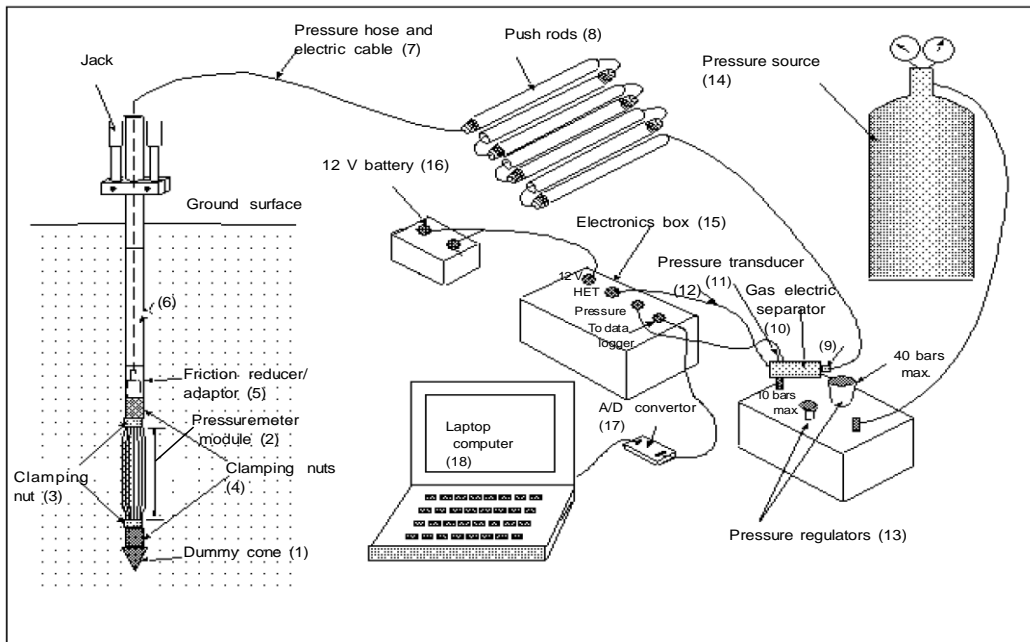


Fig. 6: The APMT equipment on site assembly [6].

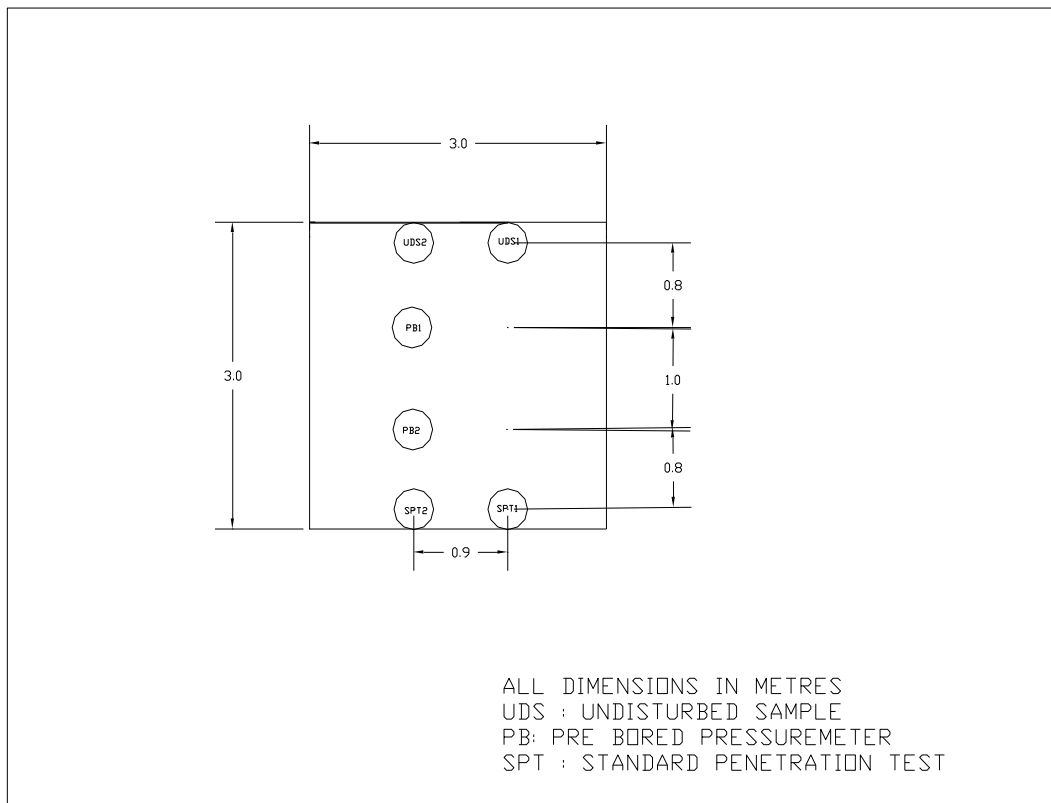


Fig. 7: Field testing plan.

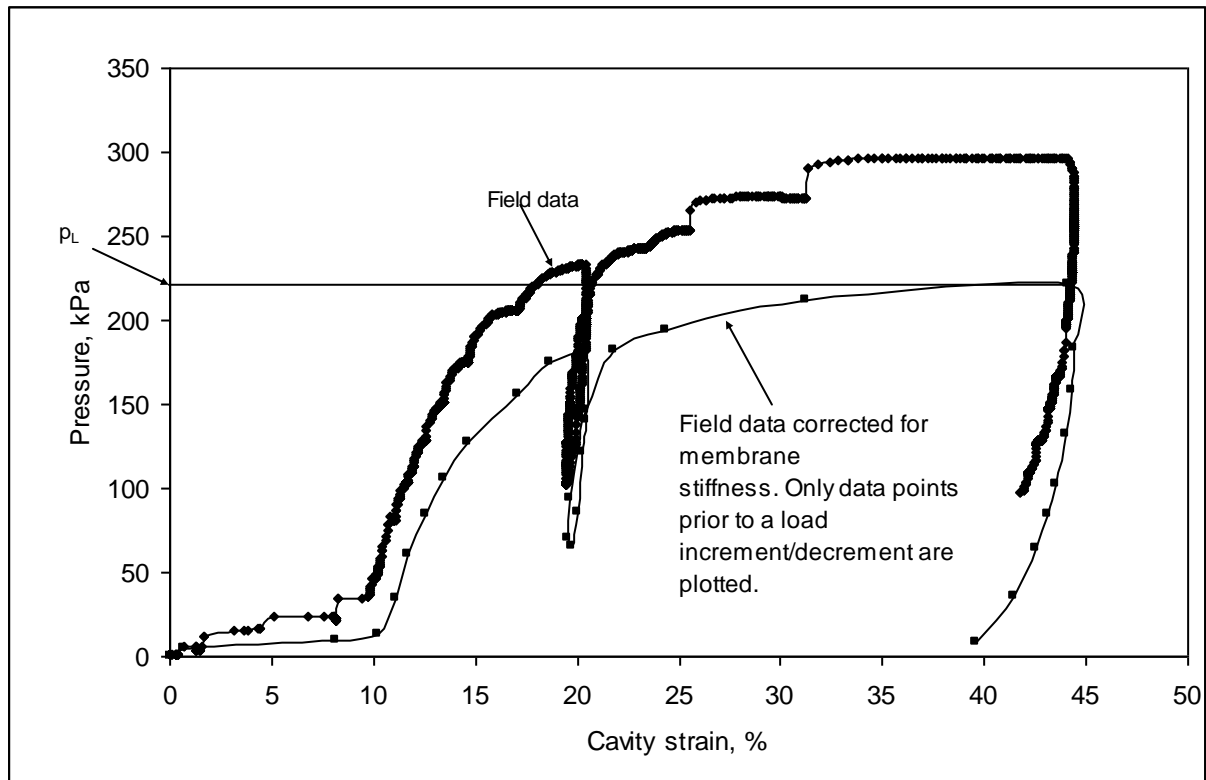


Fig. 8: Typical applied pressure-cavity strain curves at 2.0 m depth.

Table 1: Summary of classification, SPT and unconfined compression tests

Location: Open area, Civil Engineering Department, University of Engineering & Technology, Lahore												
Technique	Depth (m)	LL (%)	PI	Gravel (%)	Sand (%)	Silt/clay (%)	N value	Soil type	NMC (%)	$\gamma_d$ (kN/m <sup>3</sup> )	$s_u$ (kPa)	$E_{UCT}$ (kPa)
1	2	3	4	5	6	7	8	9	10	11	12	13
SPT1	1	25	5	0	30	70	2	CL-ML	-	-	-	-
	2	27	5	0	17	83	3	CL-ML	-	-	-	-
	3	28	5	0	20	80	2	ML	-	-	-	-
	4	27	5	0	10	90	4	CL-ML	-	-	-	-
	5	28	8	0	5	95	6	CL-ML	-	-	-	-
SPT2	1	27	7	0	13	87	2	CL-ML	-	-	-	-
	2	28	7	0	12	88	3	CL-ML	-	-	-	-
	3	28	5	0	9	91	2	CL-ML	-	-	-	-
	4	27	7	1	8	91	3	CL-ML	-	-	-	-
	5	29	5	4	5	91	6	ML	-	-	-	-
UDS1	1	22	7	0	32	68	-	CL-ML	13.6	16.7	29	67
	2	28	9	0	17	83	-	CL	20.1	16.0	44	31
	3	26	7	0	19	81	-	CL-ML	22.4	15.4	38	67
	4	32	11	0	1	99	-	CL	25.9	16.0	45	33
	5	28	8	26	12	62	-	CL	21.7	17.1	48	41
UDS2	1	29	10	0	12	88	-	CL	18.2	16.6	30	38
	2	26	9	0	21	79	-	CL	33.8	14.1	35	43
	3	28	8	0	20	80	-	CL	20.8	16.5	32	27
	4	27	7	5	5	90	-	CL-ML	20.7	17.1	32	29
	5	31	8	0	5	95	-	CL	22.5	16.4	51	43

increment controlled tests were carried out, which is a common procedure for testing with self-boring pressuremeter, full-displacement pressuremeter [10] and the Ménard pressuremeter. The pressure increments of about 25 kPa each were maintained for 1 minute with data recorded at every 1 second. The unloading was carried out at an expansion of about 45% of the initial cavity size (as arms can not move beyond this cavity strain). An unload-reload cycle was also included during loading in each test in order to estimate the shear modulus. Figure 8 shows a typical applied pressure-cavity strain curves at 2.0 m depth.

### 6. Laboratory Testing

The following tests were carried out on undisturbed and disturbed soil samples to determine the strength, stiffness and classification of soil:

- Unconfined Compression Testing (ASTM D2166)
- Grain Size Analysis (ASTM D422)
- Liquid Limit Test (ASTM D4318)
- Plastic Limit Test (ASTM D4318)

Table 1 presents a summary of laboratory test results. LL values range from 22 to 32 % and PI values from 5 to 11 %. The percentages of gravel, sand and silt/clay in different samples fall between 0 to 4 %, 1 to 32 % and 62 to 95 % respectively. On the basis of classification tests, the soil type ranges from low plastic lean clay (CL) to sandy silty clay (CL-ML). The natural moisture content (NMC) values are ranging from 13.6 to 33.8 %, bulk unit weight ( $\gamma_b$ ) values from 18.8 to 20.8 kN/m<sup>3</sup> and undrained shear strength ( $s_u$ ) values from 29 to 51 kPa.

### 7. Analysis of Pressuremeter Data

Figure 8 shows plots of the applied pressure and cavity strain data (uncorrected) and the same corrected for the membrane stiffness for a test at 2.0 m depth. The corrected curve shows only the data points prior to a load increment/decrement/

The hole diameter is created greater than the diameter of the probe by about 2.6 mm. At the start of a test, the membrane leaves the body of the probe at point B as shown in Figure 9. The pressure (corrected for the stiffness of the membrane) at point B, denoted by  $p_A$ , is required to overcome pressure around the probe due to water/mud in the borehole. The membrane then expands from points B to C until it is in contact with the cavity wall. The applied pressure between points C to D is insufficient to cause any significant strain within the soil. From points D to E, it is likely that the soil elements close to the membrane are loaded elastically. This elastic behaviour is due to the unloading that takes place during boring the hole. At point E, soil elements close to the membrane reach yield and start behaving plastically. During this stage, soil elements at various radial distances from the probe are in different stages. Those close to the probe are at failure and those at some distance from the probe are at the in-situ state [11]. Between these two extreme states are the plastic and elastic states.

The pressure at the start of the elastic yielding is denoted by  $p_h$ . Point E shows the on-set of the plastic yielding and the corresponding pressure is written as  $p_E$ . The lift-off pressure,  $p_F$  corresponds to the point on the pressure axis where tangents to the elastic part and initial part of the yield curve intersect.

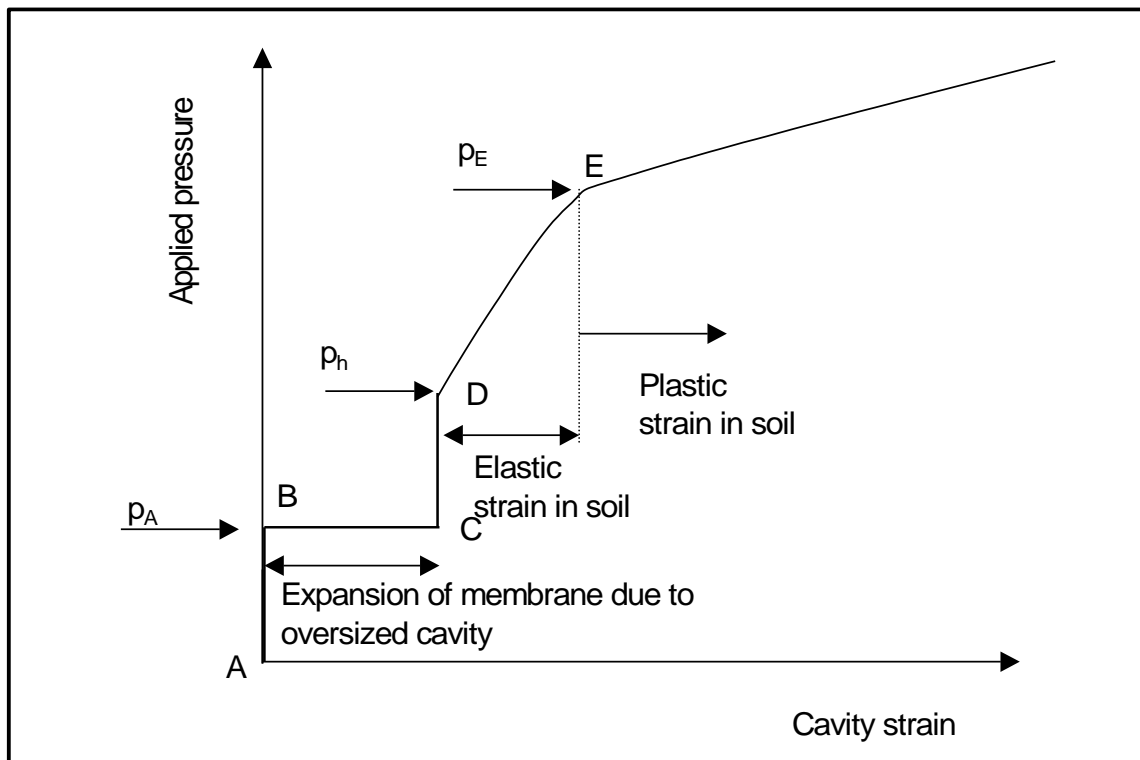


Fig. 9: An ideal stress-strain curve for the APMT.



Limit pressure ( $p_L$ ) is defined as the pressure required to double the initial volume of the cavity. Since the *HET* can record the cavity expansion strain only upto about 45%, the limit pressures have been determined by extrapolation to the maximum pressure to be reached in a *PMT* test at which the cavity will continue to expand indefinitely [9].

### 7.1 Undrained shear strength ( $s_u$ )

The undrained shear strength ( $s_u$ ) has been determined by the procedure proposed by Marsland et al. (1977) [12]. The  $s_u$  values determined according to this method are presented in column 5 of the summary Table 2. At the *PB-1* location, the  $s_u$  values range between 5 and 42 kPa and indicate soft to firm clay according to *BS 8004:1*. At the *PB-2* location, the  $s_u$  values fall between 20 and 38 kPa indicating soft to firm clay.

Figure 10 presents a comparison of undrained shear strength ( $s_u$ ) values determined from the pressuremeter and unconfined compression test (*UCT*). There are some data points showing very low  $s_u$  values from *APMT*. This is due the fact that at each *APMT* testing location, at 3 m and 5 m depths, slushy soils were present where-as the same situation was not observed at *UDS* and *SPT* locations at the same levels. Ignoring such data points, the agreement of  $s_u$

from the two sources become better. However, based on few data points no definite statement can be made.

Figure 11 shows plot of  $s_u/\sigma'_{vo}$  against depth. The  $s_u/\sigma'_{vo}$  values, in general, decrease with depth. Except four data points for soft to firm clay showing  $s_u/\sigma'_{vo}$  ratio greater than 0.8, all other ratios are less than 0.8. According to Lunne et al. (1992) [13], the subsoils with  $s_u/\sigma'_{vo} \leq 0.8$  are young clays. The soil bed tested is about one year old.

### 7.2 In-situ horizontal stress ( $\sigma_{ho}$ )

The in-situ horizontal stress,  $\sigma_{ho}$  values determined by the method proposed by Marsland et al. (1977) [12] are presented in column 4 of Table 2 and fall between 28 to 89 kPa for *PB-1* and 21 to 167 kPa for *PB-2*. The Marsland method is a graphical method and graphical methods usually do not provide exact values. The values of in-situ horizontal stress determined by this method are on higher side as compared to those determined by Aziz (2006) [14] using Akbar Newcastle Dilatometer.

The undrained shear strength can be obtained from the yield portion of the pressuremeter curve [15]. In other words the difference of limit pressure and total in-situ horizontal pressure (i.e.  $p_L - \sigma_{ho}$ ) indicates the slope of the loading curve which is a function of shear strength of a soil.

**Table 2: Summary of *APMT* test results.**

Location	Depth m	Strain range						Unload-reload cycle stiffness average	
		$p_L$ kPa	$\sigma_{ho}$ kPa	Marsland et al. (1977)		$\epsilon_{max}$ and ( $\epsilon_{max} - 0.2\%$ )		$\epsilon_{min}$ and ( $\epsilon_{min} + 0.2\%$ )	
				$s_u$ kPa	First unloading	Final unloading	Reloading	Cycle slope MPa	$G_{ur}$ MPa
		3	4	5	6	7	8	9	10
PB-1	1	309	54	35	9.9	5.5	9.2	18.9	9.5
	2	221	91	26	4.9	2.6	4.9	8.9	4.5
	3	91	61	5	2.5	4.2	1.0	2.3	1.2
	4	302	89	42	4.1	5.5	5.5	8.9	4.5
	5	80	28	9	1.2	4.5	1.8	3.8	1.9
PB-2	1	212	59	38	6.1	4.1	5.3	11.0	5.5
	2	222	79	33	4.8	3.2	6.7	7.5	3.8
	3	92	28	20	1.4	2.4	2.1	3.2	1.6
	4	364	167	38	11.8	5.6	12.4	21.7	10.9
	5	131	21	20	5.1	3.8	5.2	10.5	5.3

$G_{ur} = \text{Col.9/2}$

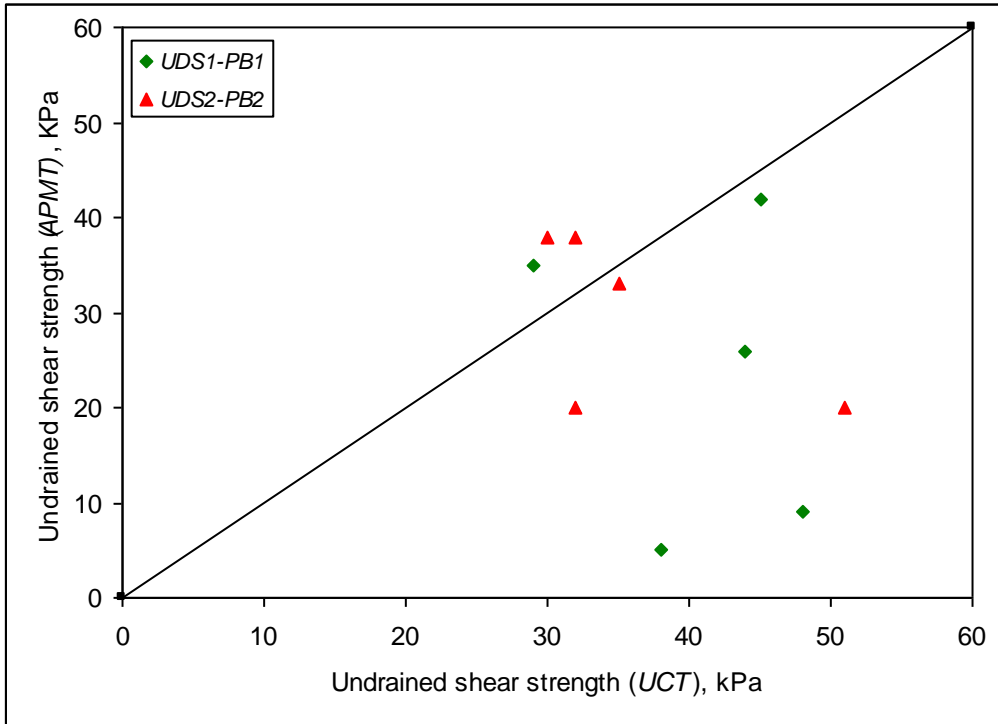


Fig. 10: Comparison of undrained shear strength from *PMT* and laboratory.

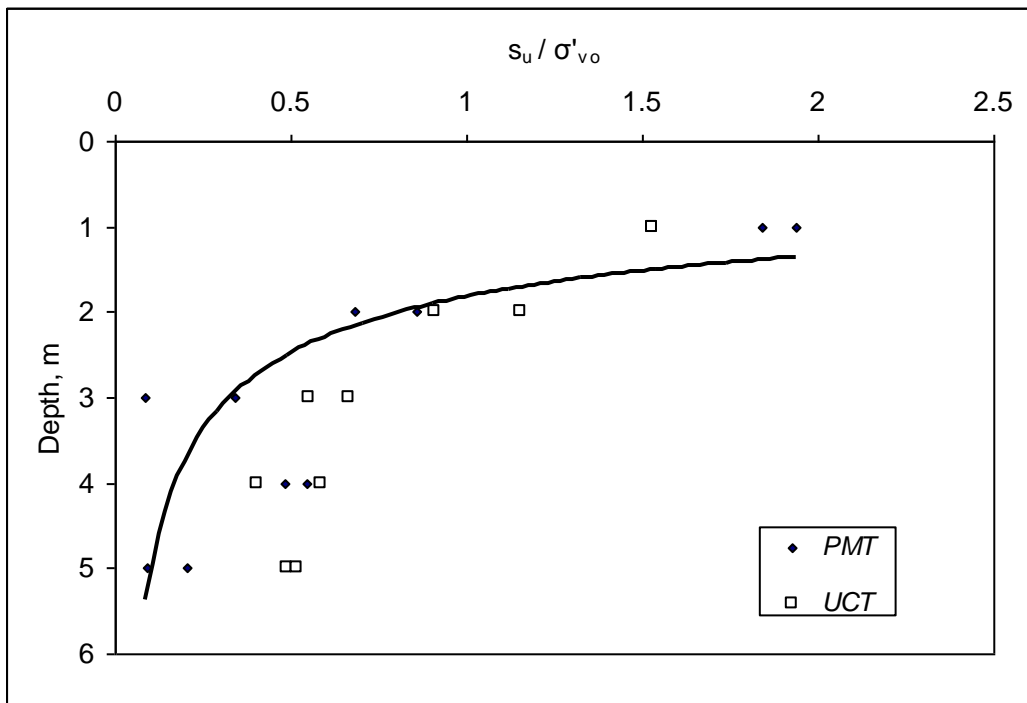
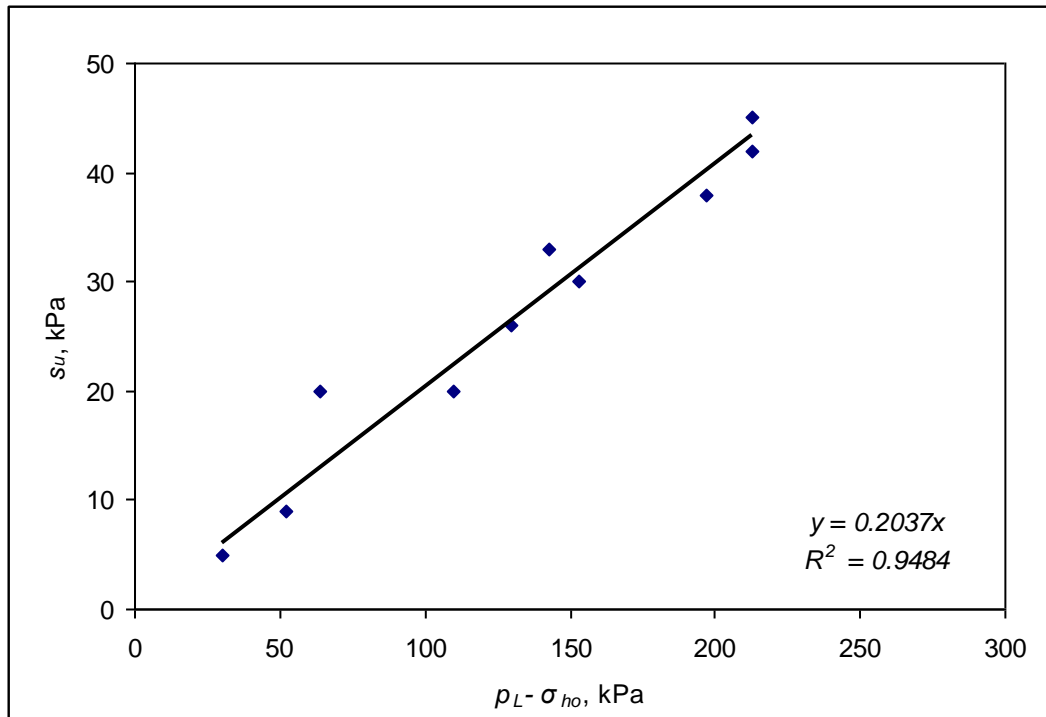


Fig.11: Profiles of  $s_u / \sigma'_{v0}$  vs depth.



**Fig. 12: Comparison between  $s_u$  and  $(p_L - \sigma_{ho})$ .**

Figure 12 shows a good agreement of undrained shear strength values against  $(p_L - \sigma_{ho})$ . The general trend of the plot, represented by the following equation, is increase in strength with increase in the difference of pressures:

$$s_u = 0.2037 (p_L - \sigma_{ho}) \quad (1)$$

Amar and Jézéquel (1972) [16] have reported coefficient 0.1818 on the right hand side of equation (1) for soft to firm clays.

### 7.3 Shear modulus (G)

Shear modulus ( $G$ ) was determined in a number of ways from the stress-strain curve. The secant shear modulus values calculated from the two unloading curves over a strain range of 0.2% (denoted by  $G_{u1}$  and  $G_{u2}$ ) are given in columns 6 and 7 of Table 2. The reloading moduli values ( $G_r$ ) for the same strain range are given in column 8 of Table 2. The average shear modulus values [17] determined from the slope of the chord of an unloading-reloading cycle (written as  $G_{ur}$ ) are shown in column 10 of the summary Table 2. The average shear modulus represents stiffness of a number of elements radiating from the probe, all being at different strain.

The profiles of shear moduli values determined from different methods are shown in Figure 13. The shear moduli values determined from different methods at the same level

are different as expected, however, an increasing trend of the shear moduli values with depth can be seen from the figure. In general, the values lie between the lower bound and upper bound as shown in Figure 13. The values in the lower and upper bound vary from 1.8 MPa to 6.2 MPa. An average trend of shear modulus values is shown by the following equation:

$$G = 0.4D + 3 \quad (2)$$

where  $D$  is the depth in m and  $G$  is in MPa.

If the Poisson's ratio,  $\nu$  is known the modulus of elasticity,  $E$  can be determined using the following relation:

$$E = 2(1 + \nu)G \quad (3)$$

Figure 14 shows the variation of the elemental secant shear modulus (final unloading) normalised with respect to the horizontal effective stress against the current cavity strain (elemental) for the PMT data. The effective horizontal stress is taken as the effective applied pressure at the start of unloading since this represents the maximum pressure to which the soil is loaded prior to unloading. The current cavity strain,  $\epsilon_{curr}$ , in Figure 14 is defined as:

$$\epsilon_{curr} = \left( \frac{\epsilon_s - \epsilon_m}{1 + \epsilon_m} \right) \quad (4)$$

where  $\epsilon_s$  is the elemental cavity strain at any point of the

cycle and  $\epsilon_m$  is the maximum cavity strain during unloading for  $G_u$ .

The results in Figure 14 show that the stiffness responses show more scatter at small strains (below about 0.3%). The scatter is reduced with strain. The early scatter may be due to consolidation taking place at the start of unloading. The large scatter in the small strain secant moduli values has also been reported by Muir Wood (1990) [17]. According to him, as it is difficult to identify precisely

the start of an unloading or reloading phase, these effects may tend to obscure the small strain behaviour of the soil.

Figure 15 shows a plot of the strain amplitude against the cycle shear modulus ( $G_{ur}$ ) normalised by the applied pressure, ( $p$ ) at the start of unloading. The plot shows that the normalized moduli are a function of the strain amplitude as expected, with a slight lower normalised modulus at higher strain amplitude. Houlsby and Nutt (1993) [18] report similar observations for the unload-reload shear modulus.

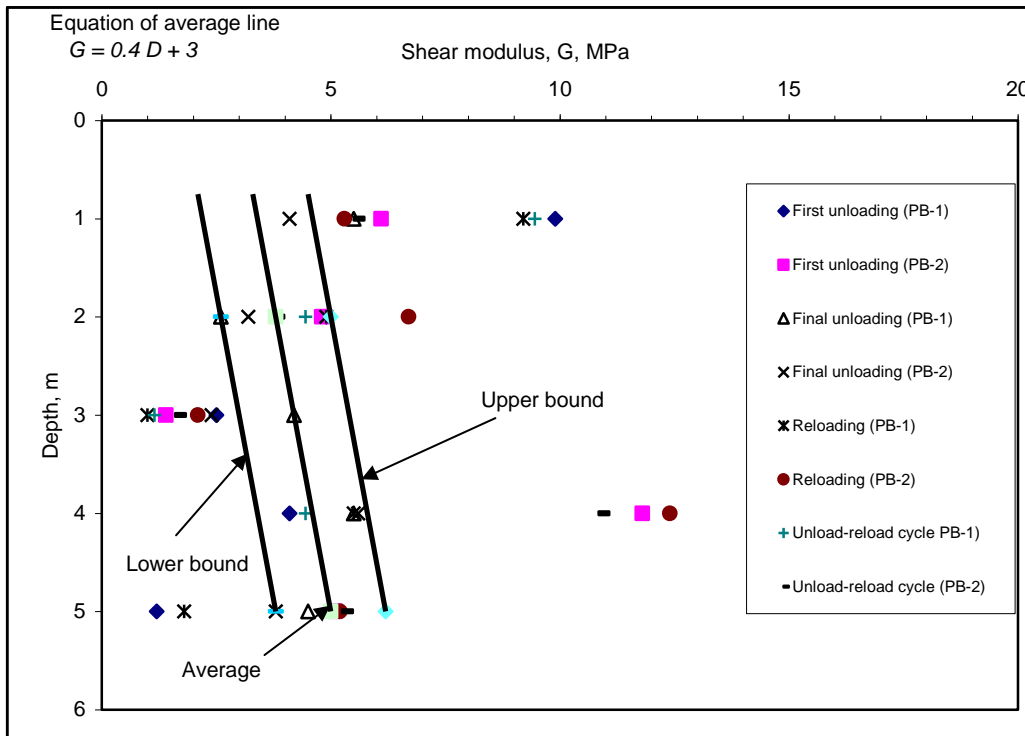


Fig. 13: Shear moduli profiles.

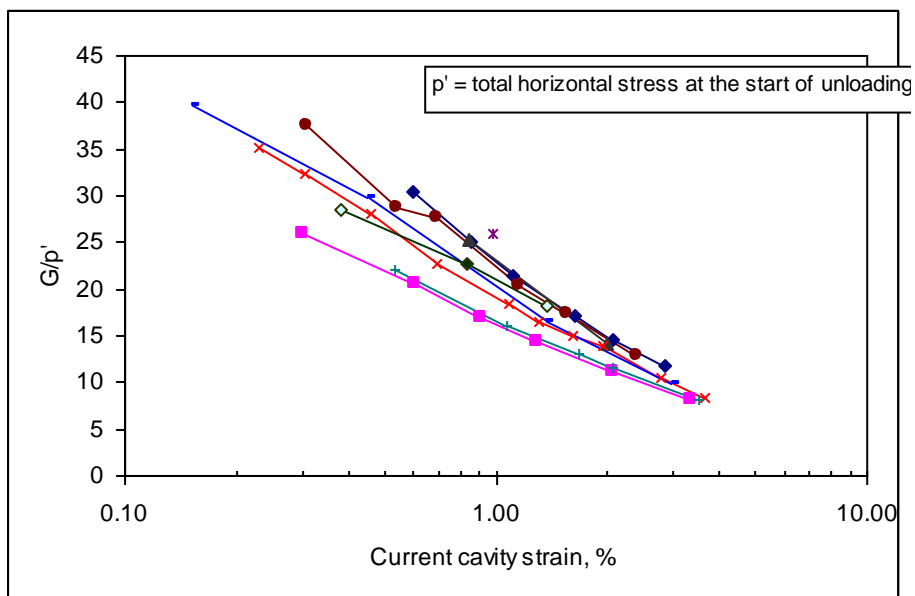


Fig. 14: Variation in elemental shear modulus with strain.

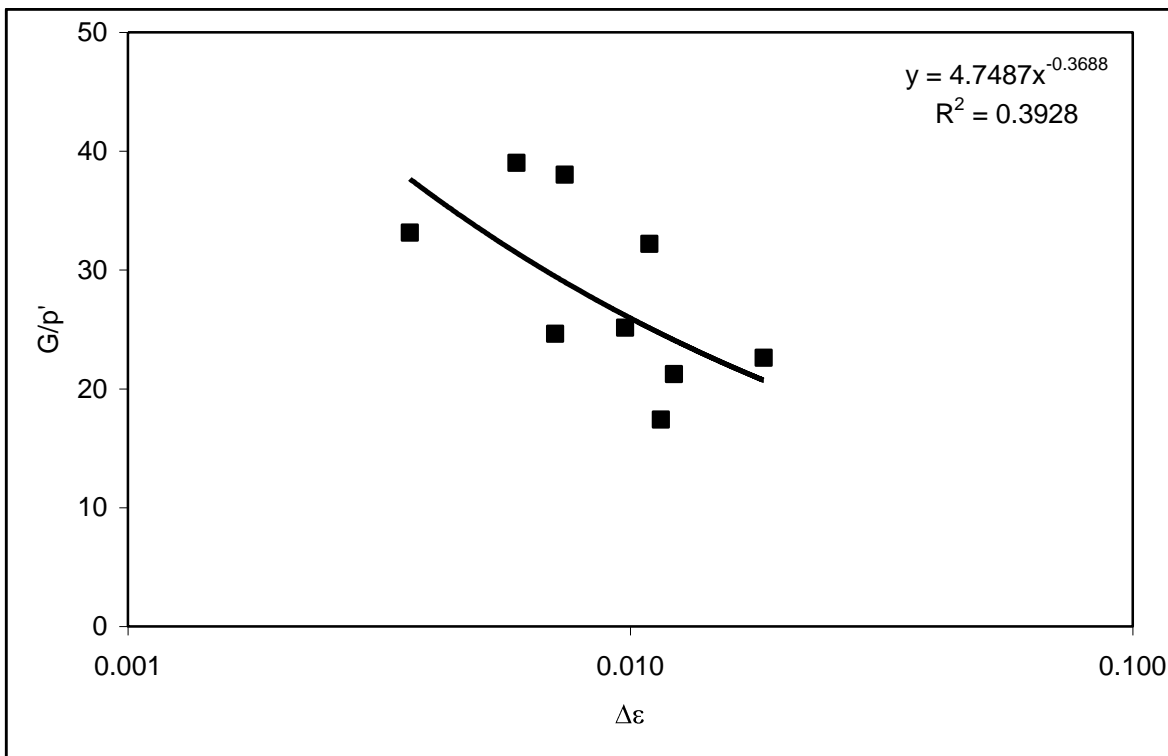


Fig. 15: Normalised shear modulus plotted against strain amplitude.

### 8. Correlations between Different Parameters

Using the available data correlations between different parameters have been developed by using the least square method. The developed correlations along with possible comments are given below:

- **PMT shear modulus vs. SPT N values**

The PMT interpreted shear moduli values,  $G_{PMT}$ , and  $N$  values of SPT for the same depth have been plotted in Figure 16. The general trend of the data is a linear increase in shear modulus with increase in  $N$ . The variation between these parameters can be represented by the following equation:

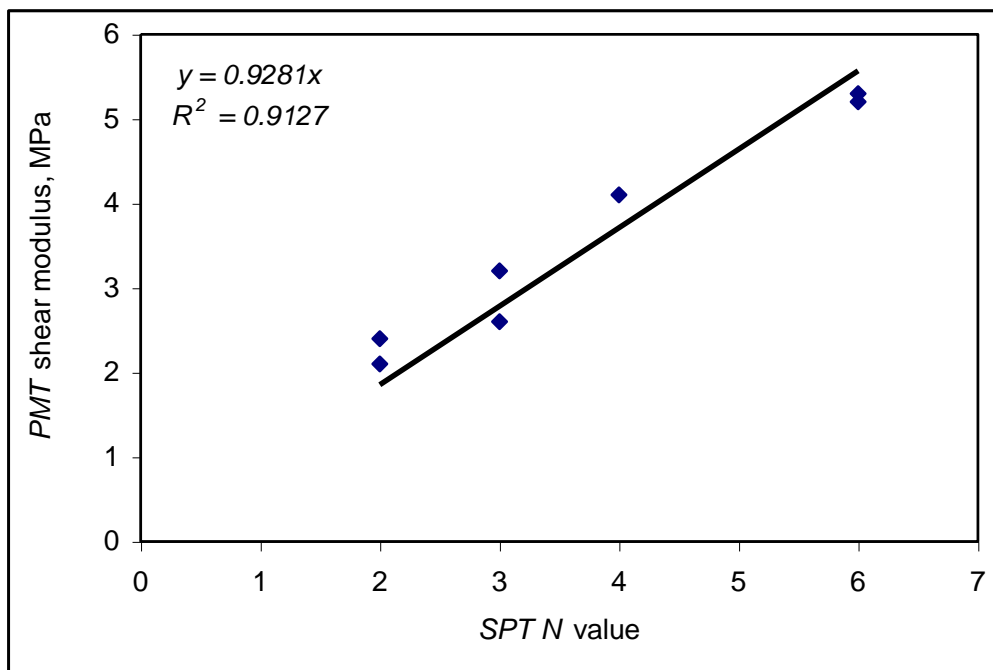


Fig. 16: Correlation between PMT shear modulus and SPT N value.

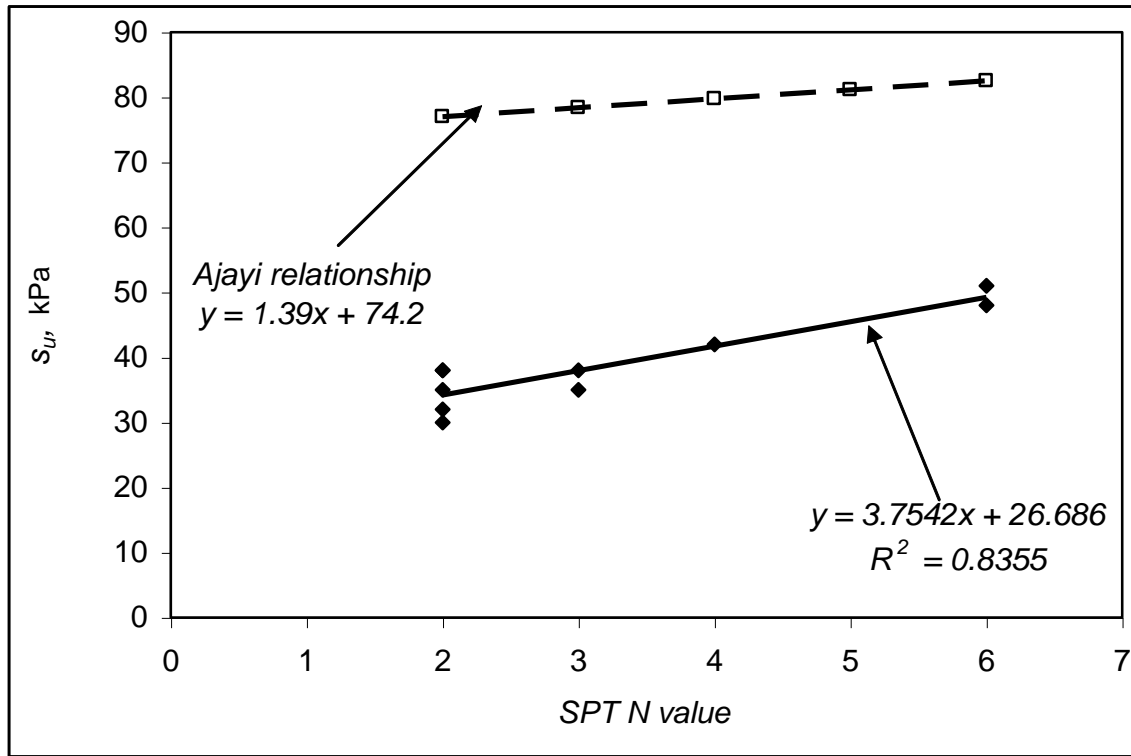


Fig. 17: Correlation between undrained shear strength and SPT N value.

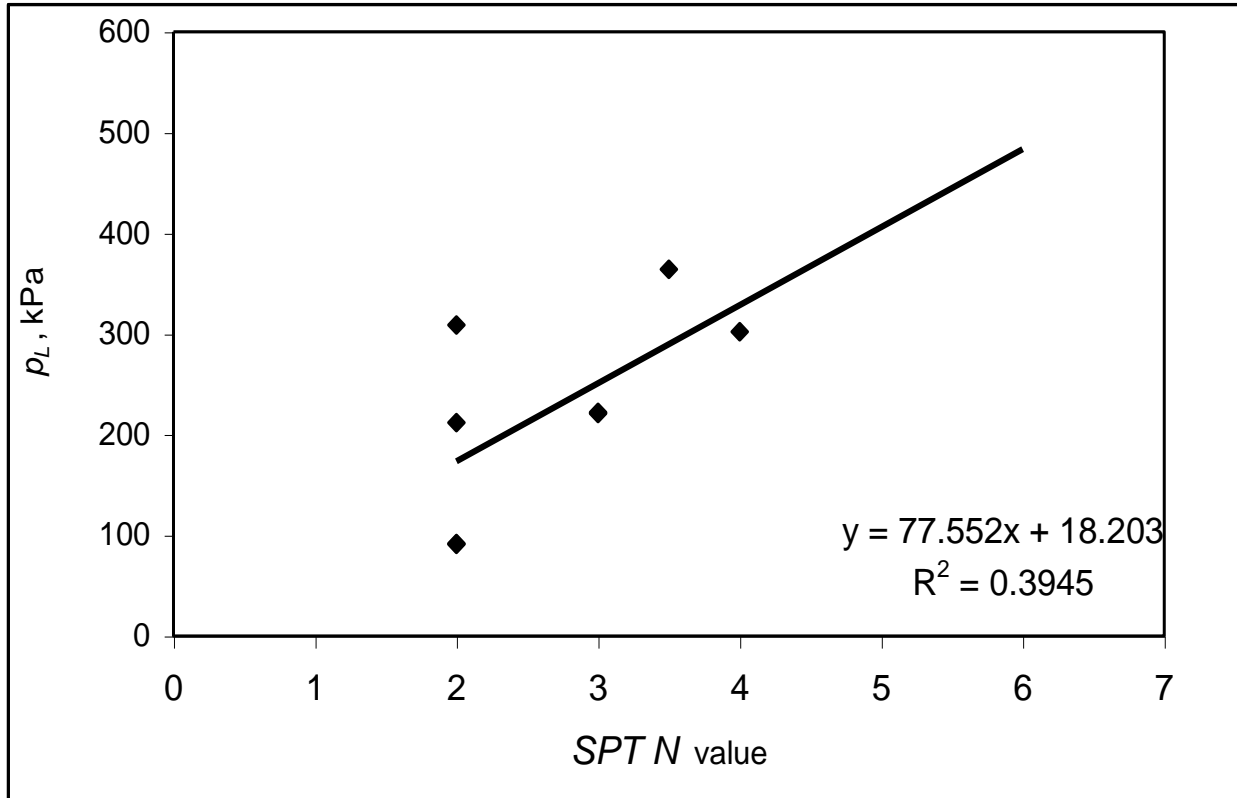


Fig. 18: Correlation between PMT limit pressure and SPT N value.

$$G_{PMT} = 0.9281 N \quad (5)$$

where  $G_{PMT}$  is in MPa.

For most clay soils  $\nu = 0.4-0.5$  [2]. Taking  $\nu = 0.45$ , equation 3 yields  $E = 2.9 G$ . By substituting the proposed value of shear modulus given by equation 5, this relation reduces to the following equation:

$$E = 2.69 N \quad (6)$$

where  $E$  is in MPa.

For the given values of  $N$ , the value of  $E$  ranges from 5.38-16.14 MPa for soft to firm clays. Bowles (1996) [2] suggests a range of 5-25 MPa for soft clays.

### • Undrained shear strength vs. SPT N values

Figure 17 presents plots of undrained shear strength against SPT N values. The general trend is linear increase in undrained shear strength with increase in SPT N values. A regression analysis yields the following equation:

$$s_u = 3.7542 N + 26.686 \quad (7)$$

where  $s_u$  is in kPa.

A comparison of the proposed relationship given by equation 7, and that by Ajayi et al. (1988) [19] is provided in Figure 17. The data points plot on or near straight line whose slope is different from that of Ajayi et al. The difference in slope may be due to the fact that Ajayi's relationship is for soils ranging from CL to CH and the proposed relationship is for CL to CL-ML

### • Limit Pressure Vs SPT N Values

Figure 18 presents plots of PMT limit pressure against SPT N values. The general trend is increase in limit pressure with increase in SPT N values. However, due to scatter in data points, it is not possible to develop some good relationship. Nevertheless, a regression analysis yields the following equation:

$$p_L = 77.552 N + 18.203 \quad (8)$$

where  $p_L$  is in KPa.

## 9. Conclusions

A pressuremeter has been developed and tested as a pre-bored pressuremeter successfully in cohesive soils varying in consistency from soft to firm. The data obtained from this PMT have been analysed using the available cavity expansion theory. The soil parameters derived from the PMT data compare well with those determined from the laboratory testing. The correlations developed between different parameters provide a good comparison with the similar previous correlations. Moreover the operation of the locally developed instrument is simple and the instrument is cost effective. With these characteristics, this instrument can

be used on projects of any size. However, further testing should be carried out to check its robustness in hard/dense soils and sands.

## REFERENCES

- [1] W. S. Kaggwa, M. B. Jaksa and R. K. Jha; *Development of Automated Dilatometer and Comparison with Cone Penetration tests at the University of Adelaide, Australia, Advances in Site Investigation Practice*, Thomas Telford, London, (1996)
- [2] J. E. Bowles; *Foundation Analysis and Design, 5<sup>th</sup> ed.* McGraw Hill Book Company, New York, (1996)
- [3] P. K. Robertson; *In Situ Testing and Its Application to Foundation Engineering*, Canadian Geotech. J., Vol. 23, No.4, (1986), 573-594.
- [4] N. J. Withers, L.H.J. Schaap and C. P. Dalton; *The Development of a Full Displacement Pressuremeter, The Pressuremeter and its Marine Applications: Second International Symposium. ASTM STP 950*, (1986), 38-56
- [5] H. M. Zuidberg and M. L. Post; *The Cone Pressuremeter: An Efficient Way of Pressuremeter Testing*, Proc. 4<sup>th</sup> Int. Symp. on Pressuremeter Testing (ISP4), "The Pressuremeter and its New Avenue" Balkema, (1995), 387-394
- [6] A. Akbar; *Development of Low Cost In-situ Testing Devices*, Ph.D. Thesis, Department of Civil Engineering, University of Newcastle, Newcastle Upon Tyne, UK, (2001)
- [7] A. Akbar, B. G. Clarke and P. G. Allen; *A Low Cost Newcastle Full-Displacement Cone Pressuremeter*, UET Research Journal, Vol. 14, Jan. 2003, Nos. 1-2, (2003), 21-25
- [8] A. Akbar, M. Arshad and B. G. Clarke; *Site Characterization Using CPT, DMT, SPT and Laboratory Test Results*, Proceedings, International Conference on Geotechnical and Geophysical Site Characterization, Taipei, Taiwan, (2008), 251-256
- [9] B. G. Clarke; *Pressuremeters in Geotechnical Design*, Blackie Academic and Professional, London, (1995)
- [10] B. G. Clarke; *Pressuremeter Testing in Ground Investigation, Part I-Site Operations*, Proc. Instn. Civ. Engr. Geotech. Engg. 119, April (1996), 96-108
- [11] G. T. Houlsby and N. J. Withers, *Analysis of the Cone Pressuremeter Test in Clay*, Geotechnique 38, No. 4, (1988), 575-587.
- [12] A. Marsland and M. F. Randolph; *Comparisons of Results from Pressuremeter Tests and Large In-situ Plate Tests in London Clay*, Geotechnique 27, No. 2, (1977), 217-243

- [13] T. Lunne, S. Lacasse and N. S. Rad; *General Report: SPT, CPT, Pressuremeter Testing and Recent Developments in In-Situ Testing*, Proceedings, 12<sup>th</sup> International Conference on Soil Mechanics and Foundation Engineering, Vol. 4, Rio de Janeiro, (1992), 2339-2403
- [14] M. Aziz; *Calibration of Newcastle Dilatometer in Cohesive Soil*, M.Sc. Thesis, Department of Civil Engineering, University of Engineering and Technology, Lahore, Pakistan, (2006)
- [15] G. E. Bauer and A. Tanaka; *Penetration Testing of a Desiccated Clay Crust*, Penetration Testing, ISOPT-1, De Ruiter (ed.) Balkema, Rotterdam, (1988), 477-488
- [16] S. Amar, and J. F. J  s  quel; *Essais en place et en laboratoire sur sols coh  rent comparaison des r  sultats*, Bull.de Liaison de LCPC, Paris, No. 58, (1972), 97-108
- [17] D.Muir-Wood; *Strain Dependent Moduli and Pressuremeter Tests*, Geotechnique, 40(26), (1990), 509-512
- [18] G. T. Houlsby and N. R. F. Nutt; *Development of the Cone Pressuremeter*, Predictive Soil Mechanics, Proc. Wroth Memorial Symp., Oxford, (1993), 254-271
- [19] L. A. Ajayi et al.; *Penetration Testing in Tropical Lateritic and Residual Soils- Nigerian Experience*, Penetration Testing, ISOPT-1, De Ruiter (ed.), Balkema, Rotterdam (1988), 315-328